arXiv:2301.10460v1 [cs.CV] 25 Jan 2023

HAL3D: Hierarchical Active Learning for Fine-Grained 3D Part Labeling

Fenggen Yu[1,2*] Yiming Qian[1] Francisca Gil-Ureta[1]
Brian Jackson[1] Eric Bennett[1] Hao Zhang[1,2]
[1]Amazon [2] Simon Fraser University

Abstract

We present the first active learning *tool for* fine-grained *3D part labeling, a problem which challenges even the most advanced deep learning (DL) methods due to the significant structural variations among the small and intricate parts. For the same reason, the necessary data annotation effort is tremendous, motivating approaches to minimize human involvement. Our labeling tool iteratively verifies or modifies part labels predicted by a deep neural network, with human feedback continually improving the network prediction. To effectively reduce human efforts, we develop two novel features in our tool, hierarchical and symmetry-aware active labeling. Our human-in-the-loop approach, coined HAL3D, achieves 100% accuracy (barring human errors) on any test set with pre-defined hierarchical part labels, with 80% time-saving over manual effort.*

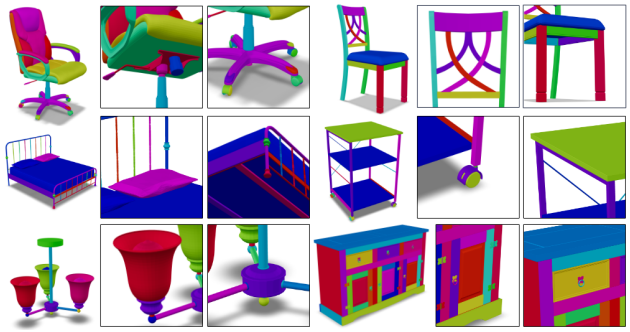


Figure 1. Fine-grained parts of the 3D models shown exhibit the kind of geometric and structural complexity and diversity that part labeling has to handle. No existing methods, whether learned or heuristic-based, could obtain close-to-fully-accurate labeling in these challenging cases, while our human-in-the-loop active learning tool can achieve 100% accuracy, minus human errors.

1. Introduction

Semantic shape segmentation and labeling [8, 24] is a classical problem with numerous applications [16], including shape/part recognition, retrieval, indexing, and attribute transfer. We consider the problem of *fine-grained* 3D part labeling, a task that has not received as much attention as the typical semantic segmentation into coarse/major parts (e.g., backs, seats, and legs for chairs). While these coarse semantic groups support high-level visual perception, they do not possess sufficient granularity to address shape properties related to motion, function, interaction, or construction. Indeed, fine-grained object parts, e.g., the individual wheels and the small mechanical parts in a swivel leg, are both function-revealing and build-aware (see Fig. 1), with strong ties to how the objects were physically assembled or virtually built by artists. Real-world applications such as product inspection, assembly, customization, and robot interaction all operate on fine-grained object parts.

Learning to label fine-grained parts is a highly challenging problem due to the great structural variations among the small and intricate parts, even for shapes that belong to the same category, as shown in Fig. 1. On a challenging dataset with average part counts per category ranging from 15 to more than 500, state-of-the-art learned models such as [30] can only achieve mean IoU scores below 50%, out of a maximum of 100% for ground truth (GT) results. Also challenging is the tremendous data annotation effort needed to train methods to segment and label fine-grained 3D parts. On the other hand, for applications which demand de facto 100% accuracy, e.g., diagnoses in medicine and quality assurance in e-commerce, one can hardly rely on a fully automatic method to reach the mark. It is arguable that the only means to guarantee full accuracy is to have humans validate all results, as in the setting for data annotation.

In this paper, we present the first *active learning* tool for fine-grained 3D part labeling. Given a set of 3D shapes segmented into fine parts, our labeling tool assigns one of the predefined labels to each part. These input parts are deemed *atomic* (i.e., indivisible); they can be as low-level as mesh triangles and as high-level as results obtained by an unlabelled semantic segmentation scheme, or mid-level components resulting from an over-segmentation. In general, active learning iterates between automated labeling and hu-

*Work done during internship at Amazon

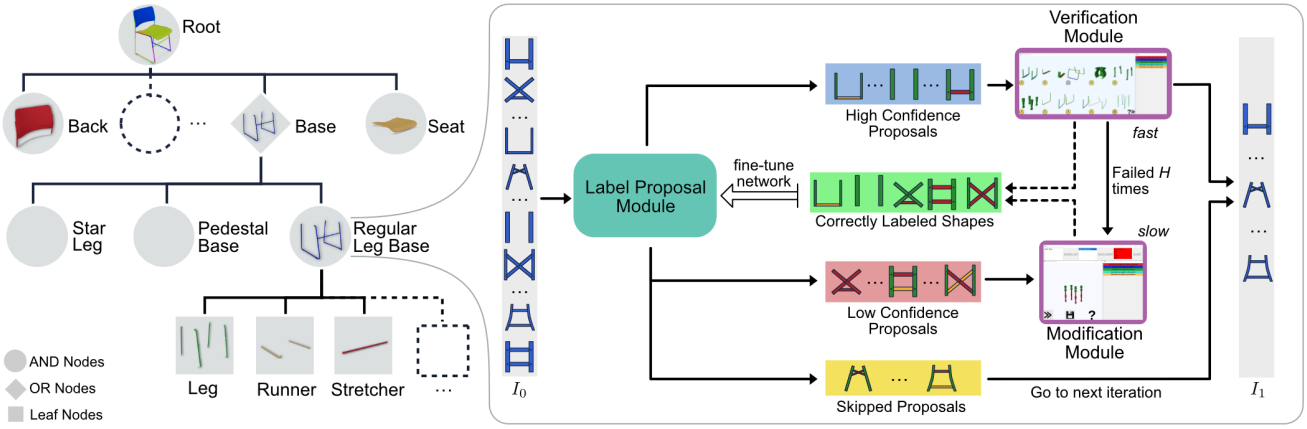


Figure 2. Our human-in-the-loop, hierarchical active learning (HAL3D) tool for fine-grained 3D part labeling. The input consists of a set of test shapes each pre-segmented into parts. The labeling proceeds hierarchically, following a tree structure (left) that organizes the hierarchical part labels, from coarse labels (top) to fine-grained labels (bottom). For a node in the label tree (with label l = "Regular Leg Base" in the illustration), the input I_0 is the subset of parts labeled l by its parent. When labeling parts with l, first the label proposal module assigns refined labels for each part. Then, proposals are sorted by label probability, with the high-confidence (HC) proposals passed to the verification module. The verification step stops once the rate of failed shapes reaches a threshold. Next, the low-confidence (LC) proposals are passed to the modification module to be corrected. Correctly labeled shapes are used to fine-tune the network. Skipped and failed shapes go to the next iteration I_1 for labeling. The iterations terminate when all shapes have passed human verification.

man input for label rectification [41]. Compared to conventional learned models with full autonomy, such a *human-in-the-loop* approach provides a viable option to achieve 100% accuracy on test sets, barring human errors.

As shown in Fig. 2, our interactive labeling tool iteratively verifies or modifies part labels predicted by a deep neural network, with human feedback continually improving the network prediction. Specifically, our system consists of three modules for label proposal, verification, and modification. Label proposals are produced by dynamic graph CNN (DGCNN) [34], with the resulting label probabilities dictating whether to pass the predicted labels to the verification or modification module. Both human-verified and corrected labels are passed back to the label proposal network to fine-tune it. The iteration terminates once all part labels have passed human verification.

As the key criterion for success with active learning is the minimization of human effort, we design and incorporate two novel features into our labeling tool:

- *Hierarchical* labeling: We organize all part labels in a tree structure, which guides our prediction-verification-modification process so that labels further down in the hierarchy are dealt with only *after* their parent labels have been fully verified. With both human users and the prediction network only needing to deal with labels at the same level of the hierarchy rather than across all levels, there is less load on the users to reduce possible errors and the prediction accuracy improves, which reduces the amount of label modifications, which are the most expensive task.
- Part *symmetry*: Since symmetric parts receive the same label, we employ detected symmetries to constrain and facilitate both label verification and modification.

Our hierarchical active learning tool is coined HAL3D. We adopt the hierarchical labels from PartNet [18] and train and test our labeling tool on both PartNet, which comes with semantic part segmentations, and Amazon-Berkeley Objects (ABO). ABO is a recently published dataset of high-quality, artist-created 3D models of real products sold online. These models are composed of build-aware connected components, but since some of these components are too coarse, we first obtain an over-segmentation of ABO models via convex decomposition and then apply HAL3D.

We evaluate the core components of HAL3D, *i.e.*, the label proposal network being fine-tuned by human feedback, and both hierarchical and symmetry-aware active labeling, by comparing to baselines and performing an ablation. The results demonstrate clear efficiency of HAL3D over labeling tools without active learning and non-hierarchical designs. Overall, HAL3D achieves 80% speed-up over manual fine-grained labeling, on the PartNet test set.

2. Related Work

Most approaches to semantic 3D shape segmentation and labeling have been designed to reason about coarse- or high-level structures and to target fully autonomy. Considerably less work has been devoted to fine-grained segmentation and labeling or human-in-the-loop approaches.

Coarse 3D shape segmentation and labeling: Since the

seminal work on learning 3D mesh segmentation and labeling [12] in 2010, many learning methods have been proposed [8]. Prominent supervised methods such as PointNet [21], PointNet++ [22], and DGCNN [34] perform feature learning over point clouds, while MeshCNN [7] develops convolution and pooling layers that operate on mesh edges. These methods, among many more, produce both parts and part labels, but they have only been trained and tested on datasets with coarse segmentations, such as the ShapeNet part [41] and the COSEG datasets [32]; most object categories therein were labeled with only 2-5 parts.

High-level parts, e.g., the legs, seats, and backs of chairs, typically possess sufficient structural consistency (e.g., in terms of relative positioning), hence predictability, to facilitate supervised learning. Most unsupervised or weakly supervised approaches also leverage such consistencies. In particular, earlier methods for co-segmentation, i.e., segmenting a *set* of related shapes altogether, all rely on alignment or clustering, either in the spatial domain [6] or feature spaces [9, 26]. More recently, resorting to DL, Ada-Coseg [46] optimizes a group consistency loss defined by matrix ranks, while BAE-Net [3] and RIM-Net [19] obtain co-segmentations by learning branched neural fields.

Fine-grained segmentation: Fine-level parts are important in many real-world applications since, whether large or small, each of them has a function to serve and often a motion to carry out. However, the structure consistency possessed by major semantic groups is mostly lost among fine parts. Such parts could be obtained via shape decomposition based on geometric properties such as convexity [11, 36], cylindricity [45], or through primitive fitting using cuboids [27, 40] or quadrics [20, 42]. However, the resulting segmentations are neither semantic nor labeled.

Most learning-based solutions are unsupervised or self-supervised, with a key reason being that annotating fine parts is an extremely tedious task. Wang et al. [30] develop deep clustering to learn part priors from training shapes with fine-grained segmentation but no part labels. As a result, no semantic labels are produced on test shapes either. Most recently, Sharma et al. [25] perform projective shape analysis [33], where a fine-grained 3D segmentation can be obtained by aggregating segmented multi-view renderings, drawing benefits from both texture cues and the ability of 2D CNNs to learn detailed image representations. Both of these methods operate fully automatically after training, but their performance falls far short of 100% accuracy: 32.6% mean IoU score achieved by [25] on PartNet [18] with fine-grained (Level-3) parts (part counts ranging from 4 to 51), and below 50% mean IoU by [30] on a more challenging dataset with part counts ranging from 15 to 500+.

Instead of operating on low-level shape elements such as points [30] and pixels [25], the neurally-guided shape parser [10] (NGSP) is trained to assign fine-grained semantic labels to *regions* of a 3D shape with improved labeling accuracy: mean IoU score up to 58% on PartNet. NGSP parses region label proposals generated by a guide neural network using likelihood modules to evaluate the global coherence of each proposal. It is still designed as a fully automatic method, but the authors did suggest the need for human-in-the-loop approaches to "scale beyond carefully-curated research datasets to 'in-the-wild' scenarios."

Hierarchical analysis: A fine-grained shape understanding is also attainable via hierarchical structural analysis. Some early works perform rule-based reasoning to construct symmetry hierarchies [35] and shape grammars [15], while others work with geometric priors, e.g., convexity [2], for hierarchical shape approximation. Similar to fine-grained segmentation, most learning-based approaches to hierarchical structural analysis are also unsupervised or weakly supervised, including co-hierarchical analysis [29], hierarchical cuboid abstraction [27], recursive implicit fields [19], and inverse constructed solid geometry modeling [13, 42]. All of these methods are designed to be full automatic and work well only with shallow hierarchies.

Active learning for part labeling: The classical and core question for active learning [1, 23, 43] is: "How does one select instances from the underlying data to label, so as to achieve the most effective training for a given level of effort?" Past works have studied uncertainty and diversity for interactive segmentation and labeling of 3D shapes [5, 32], medical images [28], and large-scale point clouds [38], to name a few. We utilize active learning as a means to achieve 100% labeling accuracy, regardless whether the test shapes belong to a "research dataset" or are "in-the-wild."

Most closely related to our work is the active framework for region annotations by Yi et al. [41]. Both works share the common goal of producing accurate, human-verified labels. On the other hand, their work imposes a fixed human effort budget, while ours does not. Technically, their work relies on a conditional random field to automatically propagate human labels, while our work integrates a DL module [34] into an active part labeling tool. The only prior work that combines deep and active learning for 3D segmentation [5] focuses on boundary refinement, just as the earlier work [32] whose learning module is constrained k-means clustering. However, none of these tools were designed to work with fine-grained labels, e.g., still only four part labels for the chair category [5, 32, 39, 41].

Finally, while our work is the first active learning tool for fine-grained 3D part labeling, hierarchical active learning has been employed in other data domains such as documents. In hierarchical text classification [4, 14], text labels can also be organized hierarchically. In comparison, semantic labeling of 3D parts in a shape collection poses various challenges including richer structural variations, part relations, and more costly and delicate user interactions.

3. Method

Given a shape test set S, where each shape is pre-segmented into parts, our methods assigns a label $l \in L$ to each part of each shape. The set of labels, L, is predefined and organized in a tree structure such that coarse labels are at the top, and fine-grained labels at the bottom. The labeling progresses hierarchically top-to-bottom, assigning first coarse labels and refining them at each step, achieving high-accuracy fine-grained labeling results.

At each node, we use an active learning based tool to iteratively engage human interactions into the part labeling process. With this tool, we obtain a labeling accuracy close to 100%, minus human errors, on each node.

3.1. Hierarchical labeling strategy

Inspired by PartNet [18], we organize the part labels into a tree structure based on their semantic definitions. Our tree structure has two types of nodes: an "AND" *internal* node indicates "what part(s) it has" (e.g., the regular base has legs and a runner), while an "OR" node indicates "what type it is" (e.g., the base is of type star or pedestal). The labeling on "AND" nodes is done based on part features, while the labeling on "OR" nodes is based on group features; see Fig. 3. Each leaf node presents a final part label.

At each node of the tree, we combine a deep neural network with an active learning tool to perform part labeling. Consider a single shape $s_i \in S$ and its set of parts P_i. At the root node, the input are all the parts of shape s_i, that is $P_{root} = P_i$. After finishing the labeling task at the root node, the set of parts is split into one or more subsets $P_l \subseteq P_{root}$ corresponding to the children labels l. Then, each subset is input to the respective node for further labeling. By splitting the input set at each node, the size of the input decreases as the depth of the node increases. Finally, the labeling stops when we reach a leaf node.

The complexity of our labeling scheme depends on the structure of the tree. On one extreme, if all labels are direct children of the root node, training of the root node would be more complex but we would only train one node. The other extreme is a binary tree, where each node is trained to distinguish between just two labels, but we have to train several nodes increasing the total training time. In particular, we found that PartNet's trees tend to have too many internal nodes. For our trees, we modify the initial tree structure from PartNet using a heuristic rule: we remove internal "AND" nodes which contain less than three children and keep all "OR" nodes. This way, our tree structure is better balanced for our task. Examples of our modified tree structures are provided in the supplementary material.

3.2. Symmetry-assisted labeling

Another novel feature to accelerate HAL3D makes use of detectable part symmetries on the test set. Symmetry is ubiquitous in man-made objects and it is common practice for 3D artists to copy-and-paste symmetric or repeated parts when building 3D assets. Symmetry detection has been a well-studied subject in geometry processing [17] and there are a variety of applicable techniques. For simplicity, we simply use sizes of the part oriented bounding boxes as a crude and conservative feature to detect part symmetries.

As symmetric parts are expected to share the same label, we accelerate our active learning in two ways: if a proposal assigns different labels to symmetric parts, we automatically remove it from the "HC (High confidence)" set. Then, in the modification module, the user only needs to label one part of the symmetry group and our system automatically propagate it to the other parts. These features improve labeling efficiency by 20%; see Section 5.2.

3.3. Active labeling of fine-grained 3D parts

Fine-grained 3D shape segmentation and annotation is challenging because of the wide structural diversity found in small and intricate parts of each shape. This diversity makes it difficult for existing DL methods to achieve high prediction accuracy. On the other side, active learning techniques are commonly used by researchers to improve the performance of the learned classifier with the help of human efforts. We adopt these techniques and, at each node of our hierarchical labeling strategy, we use a deep active learning based method to achieve high part labeling accuracy. Our method comprises three main modules: the DL-based part label proposal network, the part label verification module, and the part label modification module.

Consider a node l in our tree structure, given the subset of parts labeled l of each shape, we iteratively update the part labels until they all pass human verification. At each iteration, we first use a DL-based neural network to make part label proposals based on part label probabilities. Then, the HC proposals are passed to the part label verification module for human verification. Next, we collect the LC, i.e., low-confidence, proposals, which are more likely to be inaccurate, and pass them to the label modification module. Finally, the verified proposals and modified proposals are combined and feed back to the proposal network to fine-tune the network weights. The active learning iteration will stop if the number of left shapes are less than 40. We explain next how we make HC vs. LC proposals.

Label proposal network. Given a subset of parts for each shape $s_i \in S$, we first sample $N = 8192$ points from the part's surface and input it into our proposal network. As is shown in Fig. 3, our proposal network uses the edge-convolution module from DGCNN to extract point features, from point cloud, and the point feature dimension K=512 . At the "AND" node, different from DGCNN which is the SOTA method to predict point labels based on point features, we use extra max-pooling operations to aggregate the

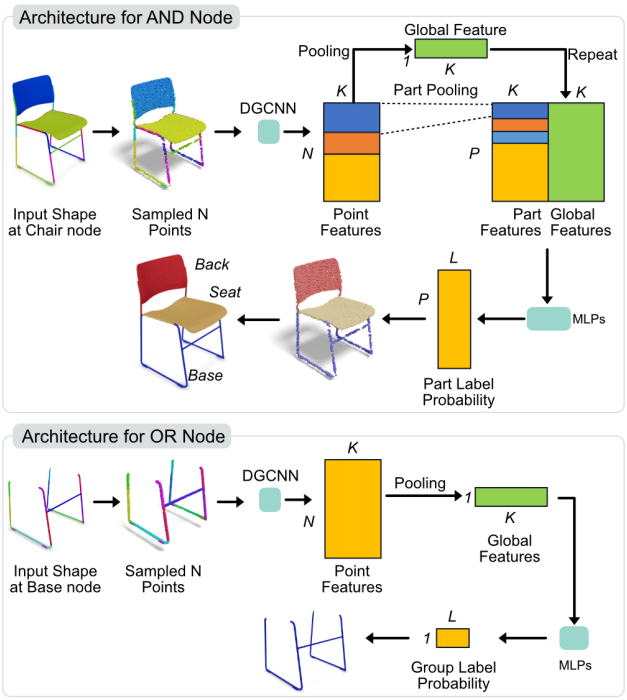


Figure 3. Label proposal architectures. Part label prediction is based on global and local, part-level features at the "AND" nodes and global features only for the "OR" nodes. The "AND" nodes would serve to predict the label for each part and the "OR" nodes would predict labels for the entire input shape. Notion-wise, N is the number of points, P is the number of parts, K is the feature dimension, and L is the number of labels.

local part features and global shape features, and input the concatenate features into the part classifier which contains 3 layers MLPs to predict part labels. Details of the network will be given in the supplementary material. As for the "OR" node, the label of the input shape will be predicted based on the global feature only, see Fig. 3. Since different shapes have different part numbers, we set the maximum part count $P_{max} = 150$ during training for batch processing and add zero-padding to the part feature matrix to make all the part feature matrices have the same size.

Label verification. Our goal is to get the labels of each shape verified by a human. To reduce verification and training times, we need to decide which shapes are verified first and how many to verify on each iteration. Shapes in the test set that have similar structure to shapes in the train set are more likely to be labeled well. We can quickly select these well-labeled shapes from the test set and use them to enhance our limited train set, improving the generalization ability of our proposal network. In our method, we first sort the test set based on predicted part label probabilities from the proposal network and arrange the test set into batches, each containing $B = 10$ shapes. Users can mark a shape as well-labeled if they see all parts are labeled correctly, or bad-labeled when one part is wrong. We design a user-friendly interface to achieve this, where users can view and rotate a batch of 3D shapes at the same time. The interface also shows the corresponding label colors for reference. Please see supplementary material for more details about our part label verification interface.

Given the sorted shapes, we need to decide how many of them to show the user before fine-tuning the prediction, to achieve a balance between processing efficiency and utilization of user feedback. To this end, we adopt an adaptive strategy: given the sorted proposals, we stop the verification step when the number of human-verified shapes on a batch is below a threshold, which is set to 4 in our experiments. This simple strategy is effective since early batches tend to have higher labeling accuracy than later batches. This way, the number of good proposals presented to the user adapts to the classification purity of the current test set.

Label modification. Shapes in the test set whose part structures and geometries differ significantly from those in the train set are less likely to be labeled accurately by the network. These shapes can be regarded as outliers in the label regression task and they can be especially valuable in fine-tuning the prediction network. Human intervention is inevitable in this situation to correct the labels. Specifically, the shapes provided to the label modification module are collected from two sets: the $Q_1 = 20$ shapes with the lowest label probabilities from the LC proposals, and those shapes that failed the user verification step more than $H = 2$ times. We feed these shapes into our part annotation interface and ask users to modify the incorrect labels.

In our part annotation interface, labels are organized hierarchically so users can quickly look up the correct labels. The label-to-color mapping table is also provided to help find the incorrect labels. More details about this interface are provided in the supplementary material.

4. Datasets and Metrics

Datasets. The Stanford PartNet [18] dataset is a common choice for fine-grained shape analysis [10, 25, 31]. We follow NGSP [10] and use the four major categories from PartNet for evaluation: chair, table, lamp, and storage furniture. Fine-grained labels in PartNet are organized into three granularity levels, and we adopt the second level in our experiments as in NGSP [10]. We first filter out noisy shapes with erroneous labels and then take 500 shapes from each category and split them into 50/50/400 as train/val/test sets.

We also evaluate HAL3D on the recent Amazon Berkeley Objects (ABO) dataset, which is composed of about 8,000 high-quality 3D shapes created by artists from real product images, where each 3D model is a combination of build-aware connected components. Unlike the 3D shapes

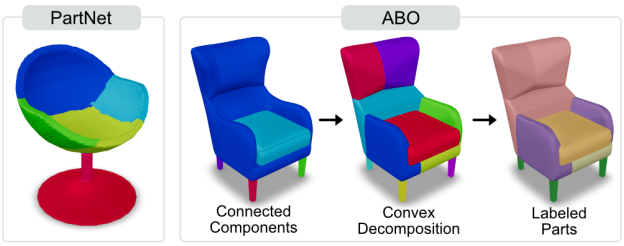


Figure 4. Comparison of pre-segmented parts in PartNet and ABO. Parts in PartNet are semantics-aware where each part has a unique semantic label. Shapes in ABO are pre-segmented into connected components where each component may corresponds to multiple labels, *e.g.*, the back and the arm of the chair are grouped into the same component, as indicated by the blue color in the second column. Instead, the part labeling operates on the convex pieces obtained by convex decomposition.

from PartNet in which each part corresponds to one single semantic label, a build-aware component from ABO may be appropriately associated with multiple labels, as shown in Fig. 4. To alleviate this issue, we apply an approximate convex decomposition [37] to further decompose each connected component into a fine-grained, i.e., over-segmented, set of convexes, where each convex piece is deemed to receive one and only one part label. Our active labeling is then applied to the set of convexes. When running the convex decomposition algorithm, we use the default parameters from the provided code, except for the concavity threshold setting, which is 0.2 in our experiments.

Since ground-truth (GT) labels are unavailable in ABO, three artists in 3D object creation are hired to help to create GT labels for each decomposed convex component. We constructed a test set containing 1,800 shapes from five categories: chair, table, lamp, storage furniture and bed.

Metrics. Active learning systems are typically evaluated from two perspectives: labeling accuracy and the amount of human efforts or involvements. We employ two standard metrics to assess the labeling quality: (1) part label accuracy measuring how many parts are correctly labeled and (2) point cloud segmentation mIoU depicting how much of the shape surface area is correctly labeled.

The amount of human efforts is measured by the consumed time in the steps of label verification and modification. Inspired from [41], we firstly give artists the same training courses and tools, and conduct user studies on PartNet. We report the total recorded labeling time in Tab. 1. We also collect the operations they used in the user study and model the total human interaction time as a function of the number of processed parts and shapes:

$$t = T_v^p(P_v, L) + T_v^f(S_v, L) + T_v^p(P_m^c, L) + T_m^p(P_m^w, L), \quad (1)$$

where P_v is the number of correctly labeled parts in verification, S_v is the number of incorrectly shapes in verification, P_m^c is the number of correctly labeled parts in modification, P_m^w is the number of incorrectly labeled parts in modification, and finally L is the total number of labels.

The function (1) is devised based on several observations: a) users need to go through and verify all the part labels in a shape to ensure that the shape is correctly labeled; b) users can easily pick up failure cases during label verification if any part of a shape is incorrectly labeled, without checking other parts; and c) users need to check all the parts in each shape to know whether it needs modification.

The right-hand functions in (1) are formulated based on the recorded time and operations from our user study:

$$\begin{aligned} T_v^p(P_v, L) &= (0.31 + 0.03 * L) * P_v, \\ T_v^f(S_v, L) &= (1.47 + 0.05 * L) * S_v, \\ T_v^p(P_m^c, L) &= (0.31 + 0.03 * L) * P_m^c, \\ T_m^p(P_m^w, L) &= (5.28 + 0.23 * L) * P_m^w, \end{aligned} \quad (2)$$

where T_v^p is the checking time for correctly labeled parts, T_v^f is the verification time for incorrectly labeled shapes, and T_m^p is the time for part label modification. We use these functions to evaluate the timing for other methods on ABO and our ablation study on PartNet.

5. Experiments

We have implemented our approach in PyTorch. The label proposal network is pre-trained with the Adam optimizer on the training set of PartNet for 250 epochs, where the learning rate is 0.001 and it is decreased by 0.8 every 25 epochs. When fine-tuning the network in HAL3D, the learning rate is fixed to 0.0001 and the epoch number is 125. Our experiments were ran on an NVIDIA Tesla V100 GPU, and the training time varies from 20 minutes to 3 hours according to the number of parts at each node.

5.1. Competing methods

We compare HAL3D, our hierarchical active labeling tool, with two automatic part labeling methods,

• **PartNet** [18], which employs the PointNet++ [22] backbone for point-wise feature extraction and labels parts by a voting scheme over points belonging to the same part.

• **NGSP** [10], which aggregates point-wise features via PointNet++ [22] to obtain part features and then leverages a likelihood-aware beam search for optimization; this represents the state of the art for fine-grained labeling.

and two variants of our labeling approach,

• **Our prop.** is one such variant without using the manual label verification or modification module; it predicts part labels using the label proposal network only.

Table 1. Quantitative comparison against the competing labeling methods and variants. In the table, "AL" indicates whether a method uses active learning. Since PartNet, NGSP, and Our prop. are automatic methods, their entries are marked with a '-' instead. "Accu." denotes the part label accuracy, "mIoU" denotes the mean Intersection-over-Union, and "Lab. time" denotes the labeling time (hours in total) for the active learning methods.

Method	AL	Accu.	mIoU	Lab. time
Chair				
PartNet [18]	-	54.90	31.04	-
NGSP [10]	-	68.98	42.90	-
Our prop.	-	67.45	41.34	-
DAL3D	✓	89.84	72.30	5.99
HAL3D	✓	94.13	84.92	4.34
Table				
PartNet [18]	-	33.21	14.92	-
NGSP [10]	-	47.11	27.94	-
Our prop.	-	42.77	23.50	-
DAL3D	✓	78.53	69.82	9.14
HAL3D	✓	84.18	74.65	4.41
Storage furniture				
PartNet [18]	-	55.82	30.86	-
NGSP [10]	-	70.60	45.79	-
Our prop.	-	69.82	42.43	-
DAL3D	✓	84.57	71.99	4.81
HAL3D	✓	93.09	88.72	3.87
Lamp				
PartNet [18]	-	38.28	11.02	-
NGSP [10]	-	49.76	23.49	-
Our prop.	-	44.77	19.27	-
DAL3D	✓	83.14	69.35	4.52
HAL3D	✓	90.53	79.51	2.16

• **DAL3D** is a deep active learning variant of our approach without using the hierarchical labeling strategy.

5.2. Evaluation on PartNet

All methods presented in this section are pre-trained and tested on the training and test sets of PartNet, respectively.

Quantitative comparison. Tab. 1 starts with comparing the three automatic methods (PartNet, NGSP, and our label proposal network), where PartNet is inferior to both NGSP and our method due to its hand-crafted voting mechanism. Our simple network achieves comparable accuracy compared to NGSP (difference by 0.11 and 3.49 with respect to mIoU and part accuracy, respectively). However, NGSP suffers from significantly longer running time due to the intensive beam search; see the supplementary for a running time comparison. In contrast, our proposal network is effective and efficient, *i.e.*, capable of quickly producing accurate initial labels to reduce the manual workload in verification and modification for active learning.

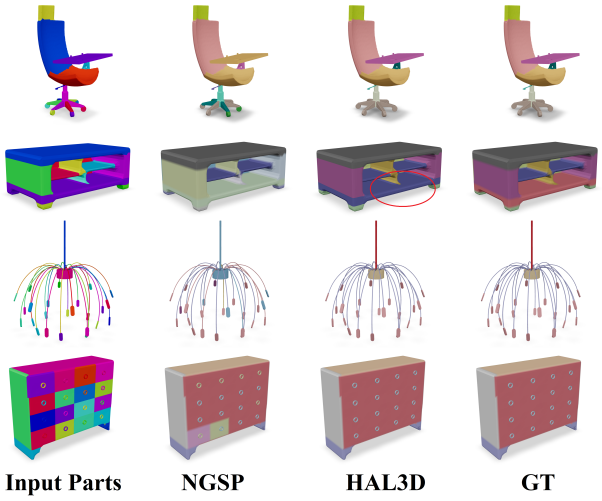


Figure 5. Visual comparison between labeling methods. HAL3D can achieve results approaching GT, barring human errors. The only mis-labeled part by HAL3D here is the bottom panel of the table (red oval), which could be easily labeled as shelf by users.

Table 2. Ablation study on key modules of HAL3D for chair category. The last column "Lab. time" denotes total labeling time.

Row ID	Prop.	Hier.	Sym.	Lab. time (hours)
2nd	-	-	-	22.05
3rd	✓	-	-	8.65
4th	✓	-	✓	5.99
5th	✓	✓	-	5.21
6th	✓	✓	✓	4.34

The results in Tab. 1 also show that even with the sophisticated design in NGSP, the highest accuracy attained is only 70%. Hence the performance of automatic fine-grained labeling methods still falls far below that of active learning methods with human supervision, where the largest and smallest accuracy gap is 40.77% and 22.49% between NGSP and HAL3D, respectively.

HAL3D consistently outperforms our DAL3D variant in all metrics, particularly 2.42 hours faster on average on labeling time, demonstrating the importance of our hierarchical labeling order for reducing manual workload. We also provide qualitative comparison in Fig. 5.

Ablation study. Tab. 2 verifies the contribution of the main components of HAL3D on minimizing human labeling efforts, a key criterion for success for a human-in-the-loop approach. The second to fourth columns indicates:

• **Prop.** if the label proposal network is used;

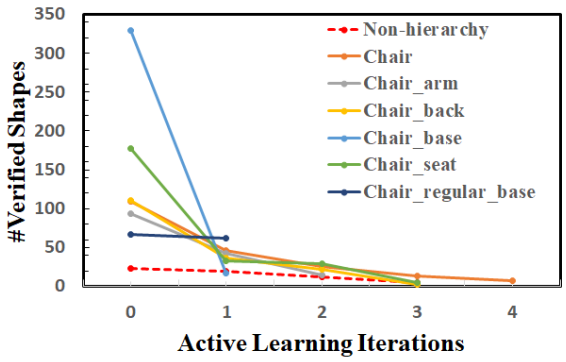


Figure 6. A plot of the number of human-verified shapes (max = 400) at different nodes (only those which existed in more than 100 shapes) of the chair category. The plot shows that with hierarchical active learning, many more shapes pass the verification, hence saving on the costly label modification, especially at higher hierarchy levels (i.e., earlier in the labeling iterations).

- **Hier.** if the hierarchical labeling strategy is used;
- **Sym.** if the symmetry checking is used.

We compare our full approach against four baseline methods. The second row indicates a baseline that directly predicts labels by annotating with our label modification interface. The third row is a baseline that firstly uses the label proposal network and then manually modifies incorrect part labels. The fourth and fifth rows represent variants of HAL3D without the hierarchical labeling and the symmetry checking scheme, respectively. The results in Tab. 2 clearly justify the design choices in our method, where our full approach (last row) is the most efficient.

To further evaluate the effectiveness of our hierarchical labeling, we plot in Fig. 6 the number of shapes which passed human verification over the active learning iterations. As we can see, HAL3D consistently verified more shapes as correct at all tree nodes when comparing to the baseline that had no hierarchical design, *e.g.*, more than 300 shapes were marked as correct in the first iteration in the chair_base node. Essentially, our hierarchical verification splits the labeling task into smaller and easier tasks compared to the case of non-hierarchical design, which effectively reduces the burden arising from the subsequent and more costly modification step in terms of human effort.

5.3. Evaluation on ABO

We apply HAL3D to label our constructed test set for ABO, where the label proposal network is pre-trained on the training set of PartNet. As mentioned in Sec. 4, shapes in ABO are decomposed into convexes and HAL3D assigns a semantic label to each decomposed piece. Three artists were invited to use our HAL3D tool and interface for evaluation. Since GT labels are not provided in ABO, we inspect the labeling results from the artists via human cross validation with the final corrected labeling forming the GT.

Table 3. Comparison for different methods to pass human verification on test set of ABO. The time is in hours.

	Chair	Table	Lamp	Cabinet	Bed
# shapes	400	400	400	200	400
HAL3D					
Accu.	93.07	92.55	96.29	94.48	93.71
Time	6.46	7.41	4.38	3.34	4.51
PartNet + modification					
Time	28.25	33.94	31.53	13.35	25.02
NGSP + modification					
Time	28.30	34.32	31.56	13.22	24.90

Tab. 3 presents the quantitative evaluation results. HAL3D is capable of accurately labeling all categories with a 94% average accuracy within a range of 3-7 hours of manual annotation, demonstrating the effectiveness and efficiency of our approach. Our contribution to reduce human efforts in manual annotation becomes more significant when comparing against the last four rows in Tab. 3, where we use the same manual modification interface to directly correct the PartNet and NGSP results. Please see qualitative results of ABO in the supplementary material.

6. Conclusion

We present HAL3D, the first semantic labeling tool that is designed to operate on fine-grained 3D parts *and* achieve 100% labeling accuracy through full label verification by humans, barring human errors. Our human-in-the-loop approach is based on active learning, combining deep label prediction and human inputs which iteratively fine-tunes and improves the network prediction. Extensive experimental results demonstrate that human efforts are effectively reduced via hierarchical and symmetry-aware active labeling.

HAL3D is currently implemented with DGCNN [34] as the label prediction backbone, but it can be readily replaced by PointNet [21], which was adopted by PartNet [18] and NGSP [10], or a more performant alternative such as Point Transformer [44]. Also, aside from symmetry, inter-shape part correspondences can also be utilized to reduce labeling costs, assuming that they can be reliably obtained.

We regard our work as only a preliminary step towards deep active learning for fine-grained structural analysis of 3D shapes. A natural focus for future work is to develop a more sophisticated ranking or selection mechanism for label verification and modification to achieve the most effective training for a given level of human effort.

References

[1] Charu C. Aggarwal, Xiangnan Kong, Quanquan Gu, Jiawei Han, and Philip S. Yu. Active learning: A survey. In *Data Classification: Algorithms and Applications*, pages 571–597. 3

[2] Marco Attene, Michela Mortara, Michela Spagnuolo, and Bianca Falcidieno. Hierarchical convex approximation of 3D shapes for fast region selection. *Comput. Graph. Forum*, 27(5):1323–1332, 2008. 3

[3] Zhiqin Chen, Kangxue Yin, Matt Fisher, Siddhartha Chaudhuri, and Hao Zhang. BAE-NET: Branched autoencoder for shape co-segmentation. In *ICCV*, 2019. 3

[4] Yu Cheng, Kunpeng Zhang, Yusheng Xie, Ankit Agrawal, and Alok Choudhary. On active learning in hierarchical classification. In *Proceedings of the 21st ACM International Conference on Information and knowledge Management*, pages 2467–2470, 2012. 3

[5] David George, Xianghua Xie, Yukun Lai, and Gary KL Tam. A deep learning driven active framework for segmentation of large 3d shape collections. *Computer-Aided Design*, 144:103179, 2022. 3

[6] Aleksey Golovinskiy and Thomas Funkhouser. Consistent segmentation of 3D models. In *Proc. Shape Modeling International (SMI)*, 2009. 3

[7] Rana Hanocka, Amir Hertz, Noa Fish, Raja Giryes, Shachar Fleishman, and Daniel Cohen-Or. MeshCNN: A network with an edge. *ACM TOG*, 38(4), 2019. 3

[8] Yong He, Hongshan Yu, Xiaoyan Liu, Zhengeng Yang, Wei Sun, Yaonan Wang, Qiang Fu, Yanmei Zou, and Ajmal Mian. Deep learning based 3d segmentation: A survey. *CoRR*, abs/2103.05423, 2021. 1, 3

[9] Ruizhen Hu, Lubin Fan, and Ligang Liu. 3

[10] R. Kenny Jones, Aalia Habib, Rana Hanocka, and Daniel Ritchie. The neurally-guided shape parser: Grammar-based labeling of 3D shape regions with approximate inference. In *CVPR*, 2022. 3, 5, 6, 7, 8

[11] Oliver Van Kaick, Noa Fish, Yanir Kleiman, Shmuel Asafi, and Daniel Cohen-OR. Shape segmentation by approximate convexity analysis. 3

[12] Evangelos Kalogerakis, Aaron Hertzmann, and Karan Singh. Learning 3D mesh segmentation and labeling. *ACM TOG*, 29(4), 2010. 3

[13] Kacper Kania, Maciej Zięba, and Tomasz Kajdanowicz. UCSG-NET - unsupervised discovering of constructive solid geometry tree. In *NeurIPS*, 2020. 3

[14] Xiao Li, Da Kuang, and Charles X Ling. Active learning for hierarchical text classification. In *Pacific-Asia conference on knowledge discovery and data mining*, pages 14–25. Springer, 2012. 3

[15] Tianqiang Liu, Siddhartha Chaudhuri, Vladimir G. Kim, Qixing Huang, Niloy J. Mitra, and Thomas Funkhouser. Creating consistent scene graphs using a probabilistic grammar. *ACM TOG*, 33, 2014. 3

[16] Niloy Mitra, Michael Wand, Hao Zhang, Daniel Cohen-Or, and Martin Bokeloh. Structure-aware shape processing. In *Eurographics State-of-the-Art Report (STAR)*, 2013. 1

[17] Niloy J. Mitra, Mark Pauly, Michael Wand, and Duygu Ceylan. Symmetry in 3D geometry: Extraction and applications. 32(6), 2013. 4

[18] Kaichun Mo, Shilin Zhu, Angel X. Chang, Li Yi, Subarna Tripathi, Leonidas J. Guibas, and Hao Su. PartNet: A large-scale benchmark for fine-grained and hierarchical part-level 3D object understanding. In *CVPR*, June 2019. 2, 3, 4, 5, 6, 7, 8

[19] Chengjie Niu, Manyi Li, Kai Xu, and Hao Zhang. RIM-Net: Recursive implicit fields for unsupervised learning of hierarchical shape structures. In *CVPR*, 2022. 3

[20] Despoina Paschalidou, Ali Osman Ulusoy, and Andreas Geiger. Superquadrics revisited: Learning 3D shape parsing beyond cuboids. In *CVPR*, pages 10344—10353, 2019. 3

[21] Charles R. Qi, Hao Su, Kaichun Mo, and Leonidas J. Guibas. PointNet: Deep learning on point sets for 3D classification and segmentation. In *CVPR*, 2017. 3, 8

[22] Charles R. Qi, Li Yi, Hao Su, and Leonidas J. Guibas. PointNet++: Deep hierarchical feature learning on point sets in a metric space. In *NeurIPS*, 2017. 3, 6

[23] Pengzhen Ren, Yun Xiao, Xiaojun Chang, Po-Yao Huang, Zhihui Li, Brij B. Gupta, Xiaojiang Chen, and Xin Wang. A survey of deep active learning, 2020. 3

[24] Ariel Shamir. A survey on mesh segmentation techniques. *Comput. Graph. Forum*, 27(6):1539–1556. 1

[25] Gopal Sharma, Kangxue Yin, Subhransu Maji, Evangelos Kalogerakis, Or Litany, and Sanja Fidler. MvDeCor: Multi-view dense correspondence learning for fine-grained 3D segmentation. In *ECCV*, 2022. 3, 5

[26] Oana Sidi, Oliver van Kaick, Yanir Kleiman, Hao Zhang, and Daniel Cohen-Or. Unsupervised co-segmentation of a set of shapes via descriptor-space spectral clustering. *ACM TOG*, 30(6):126:1–126:9, 2011. 3

[27] Chun-Yu Sun, Qian-Fang Zou, Xin Tong, and Yang Liu. Learning adaptive hierarchical cuboid abstractions of 3D shape collections. 38(6), 2019. 3

[28] Andrew Top, Ghassan Hamarneh, and Rafeef Abugharbieh. Active learning for interactive 3D image segmentation. In *Int. Conf. on Medical Image Computing and Computer-Assisted Intervention (MICCAI)*, 2011. 3

[29] Oliver van Kaick, Kai Xu, Hao Zhang, Yanzhen Wang, Shuyang Sun, Ariel Shamir, and Daniel Cohen-Or. Co-hierarchical analysis of shape structures. *ACM TOG*, 32(4), 2013. 3

[30] Xiaogang Wang, Xun Sun, Xinyu Cao, Kai Xu, and Bin Zhou. Learning fine-grained segmentation of 3D shapes without part labels. In *CVPR*, 2021. 1, 3

[31] Xiaogang Wang, Bin Zhou, Haiyue Fang, Xiaowu Chen, Qinping Zhao, and Kai Xu. Learning to group and label fine-grained shape components. 37(6), 2018. 5

[32] Yunhai Wang, Shmulik Asafi, Oliver van Kaick, Hao Zhang, Daniel Cohen-Or, and Baoquan Chen. Active co-analysis of a set of shapes. *ACM TOG*, 31(6), 2012. 3

[33] Yunhai Wang, Minglun Gong, Tianhua Wang, Daniel Cohen-Or, Hao Zhang, and Baoquan Chen. Projective analysis for 3D shape segmentation. *ACM TOG*, 32(6), 2013. 3

[34] Yue Wang, Yongbin Sun, Ziwei Liu, Sanjay E. Sarma, Michael M. Bronstein, and Justin M. Solomon. Dynamic graph CNN for learning on point clouds. *ACM TOG*, 2019. 2, 3, 8

[35] Yanzhen Wang, Kai Xu, Jun Li, Hao Zhang, Ariel Shamir, Ligang Liu, Zhiquan Cheng, and Yueshan Xiong. Symmetry hierarchy of man-made objects. *Comput. Graph. Forum*, 30(2):287–296, 2011. 3

[36] Xinyue Wei, Minghua Liu, Zhan Ling, and Hao Su. Approximate convex decomposition for 3d meshes with collision-aware concavity and tree search. *ACM TOG*, 41(4), 2022. 3

[37] Xinyue Wei, Minghua Liu, Zhan Ling, and Hao Su. Approximate convex decomposition for 3d meshes with collision-aware concavity and tree search. *arXiv preprint arXiv:2205.02961*, 2022. 6

[38] Tsung-Han Wu, Yueh-Cheng Liu1, Yu-Kai Huang, Hsin-Ying Lee, Hung-Ting Su, Ping-Chia Huang, and Winston H. Hsu. ReDAL: Region-based and diversity-aware active learning for point cloud semantic segmentation. In *ICCV*, 2021. 3

[39] Zizhao Wu, Ruyang Shou, Yunhai Wang, and Xinguo Liu. Interactive shape co-segmentation via label propagation. In *Proc. of CAD/Graphics*, 2014. 3

[40] Kaizhi Yang and Xuejin Chen. Unsupervised learning for cuboid shape abstraction via joint segmentation from point clouds. *ACM TOG*, 40(4), 2021. 3

[41] Li Yi, Vladmir G. Kim, I.-Chao Shen Duygu Ceylan, Mengyuan Yan, Hao Su, Cewu Lu, Qixing Huang, Alla Sheffer, and Leonidas J. Guibas. A scalable active framework for region annotation in 3D shape collections. *ACM TOG*, 35(6), 2016. 2, 3, 6

[42] Fenggen Yu, Zhiqin Chen, Manyi Li, Aditya Sanghi, Hooman Shayani, Ali Mahdavi-Amiri, and Hao Zhang. CAPRI-Net: Learning compact CAD shapes with adaptive primitive assembly. In *CVPR*, 2022. 3

[43] Xueying Zhan, Qingzhong Wang, Kuan-hao Huang, Haoyi Xiong, Dejing Dou, and Antoni B. Chan. A comparative survey of deep active learning, 2022. 3

[44] Hengshuang Zhao, Li Jiang, Jiaya Jia, Philip Torr, and Vladlen Koltun. Point transformer. In *CVPR*, 2021. 8

[45] Yang Zhou, Kangxue Yin, Hui Huang, Hao Zhang, Minglun Gong, and Daniel Cohen-Or. Generalized cylinder decomposition. *ACM TOG*, 34(6), 2015. 3

[46] Chenyang Zhu, Kai Xu, Siddhartha Chaudhuri, Li Yi, Leonidas J. Guibas, and Hao Zhang. AdaCoSeg: Adaptive shape co-segmentation with group consistency loss. In *CVPR*, 2020. 3